Effects of miRNA-15 and miRNA-16 expression replacement in Chronic Lymphocytic Leukemia: implication for therapy

Giovanna Cutrona[1], Serena Matis[1], Monica Colombo[1], Carlotta Massucco[1], Gabriella Baio[2,3], Francesca Valdora[1,4], Laura Emionite[5], Sonia Fabris[6], Anna G. Recchia[7,8], Massimo Gentile[7,8], Carlo E. Neumaier[2], Daniele Reverberi[1], Rosanna Massara[1], Simona Boccardo[9], Luca Basso[10], Sandra Salvi[9], Francesca Rosa[10], Michele Cilli[5], Simonetta Zupo[11], Mauro Truini[9,12], Pierfrancesco Tassone[13], Massimo Calabrese[2], Massimo Negrini[14], Antonino Neri[6,15], Fortunato Morabito[7,8] , Franco Fais[1,4], and Manlio Ferrarini[16].

Affiliations:

[1]Molecular Pathology Unit, IRCCS-A.O.U. San Martino-IST, Genoa, Italy;

[2]Diagnostic Imaging and Senology, IRCCS-A.O.U. San Martino–IST, Genoa, Italy

[3]Current address: Aberdeen Biomedical Imaging Centre, University of Aberdeen, Aberdeen, UK.

[4]Department of Experimental Medicine, University of Genova, Genoa, Italy;

[5] Animal Facility, IRCCS-A.O.U. San Martino-IST, Genoa, Italy;

[6] Hematology Unit, Fondazione IRCCS Ca' Granda, Ospedale Maggiore Policlinico, Milan, Italy

[7]Hematology Unit, Department of Onco-Hematology, A.O. of Cosenza, Cosenza, Italy;

[8]Biotechnology Research Unit, Aprigliano, A.O./ASP of Cosenza, Cosenza, Italy;

[9]Division of Histopathology and Cytopathology, IRCCS-A.O.U. San Martino-IST, Genoa, Italy;

[10]Department of Science of Health (DISSAL), University of Genoa, Genoa, Italy;

[11]Molecular Diagnostic Unit, Division of Histopathology and Cytopathology, IRCCS-A.O.U. San Martino-IST, Genoa, Italy;

[12]Current address: A.O. Division of Histopathology and Cytogenetics, Ospedale Niguarda Ca'Granda, Milano, Italy;

[13]Department of Experimental and Clinical Medicine, Magna Graecia University, Salvatore Venuta University Campus, Catanzaro, Italy.

[14]Department of Morphology, Surgery and Experimental Medicine, University of Ferrara, Ferrara, Italy

[15]Department of Oncology and Hemato-Oncology, University of Milano, Milan, Italy;

[16]Scientific Direction, IRCCS-A.O.U. San Martino-IST, Genoa, Italy;

Running title: Therapeutic approach with miR-15 and -16 in Chronic Lymphocytic Leukemia

Conflict of interest:

The authors declare no conflict of interest.

Correspondence:

Franco Fais, Dep. Integrated Oncological Therapies, Director of Molecular Pathology Unit, IRCCS-AOU San Martino-IST, L.go Rosanna Benzi, 10; zip code 16132, Genoa, Italy. Phone: +39-010-5558979; Fax: +39-010-5556531; E-mail: franco.fais@unige.it.

Abstract

Chronic lymphocytic leukemia (CLL) clones are characterized by loss of a critical region in 13q14.3, [del(13)(q14)] involving the microRNA (miRNA) cluster miR-15a and miR-16-1. We have investigated the effects of replacement of miR-15a and miR-16-1. CLL cells transfected with these miRNA mimics exhibited a decrease in cell viability *in vitro* and impaired capacity for engraftment and growth in NOD/Shi-scid,γcnull (NSG) mice. No synergistic effects were observed when the two miRNA mimics were combined. The phenomena were not restricted to CLL with the del(13)(q14) lesion. Similar effects induced by miRNA mimics were seen in cells with additional chromosomal abnormalities with the exception of certain CLL clones harboring *TP53* alterations. Administration of miRNA mimics to NSG mice previously engrafted with CLL clones resulted in substantial tumor regression. CLL cell transfection with miR-15a and miR-16-1 specific inhibitors resulted in increased cell viability *in vitro* and in an enhanced capacity of the engrafted cells to grow in NSG mice generating larger splenic nodules. These data demonstrate that the strong control by miR-15a and miR-16-1 on CLL clonal expansion is exerted also at the level of full-blown leukemia and provide indications for a miRNA based therapeutic strategy.

Introduction

CLL is characterized by the monoclonal expansion of B cells expressing CD19, CD5 and CD23 and low levels of surface immunoglobulin[1]. The mechanisms underlying the disease have only been partially elucidated. In CLL, well-defined chromosomal abnormalities, such as deletions at (17)(p13.1), (11)(q22.3) or trisomy 12 (+12) are infrequent at early stages and more common in patients with more advanced disease or at relapse. Therefore, these lesions are unlikely to contribute to the initial pathogenetic mechanisms, although they may be involved in both disease progression and resistance to therapy[2-8].

The 13q14.3 [del(13)(q14)] deletion represents a remarkable exception, since it is observed in approximately 50% of cases either in a mono- or biallelic form and is also present in the early disease stages[4, 9], including monoclonal B cell lymphocytosis or MBL[10, 11], suggesting a pathogenetic role. The deletion identified involves primarily the DLEU2 gene which carries the locus of two microRNAs (miRNAs): miR-15a and miR-16-1 (miR-15 and miR-16, respectively)[12-17]. MiRNAs are single stranded, non-coding RNA, which are evolutionary conserved and capable of regulating the expression of several genes concomitantly[18]. The regulation of gene expression occurs mainly through the specific binding of miRNAs to the 3'-un-translated region (3'-UTR) of the messenger RNA of the target gene via a RNA-induced silencing complex[19], although additional mechanisms have been described[20].

Biallelic del(13)(q14) results in an incapacity of the cell to express miR-15 and miR-16 (ref. 14, 15, 17, 21, 22) (Supplementary Figure S1) and the deregulation of several target genes, including those involved in cell cycle progression and apoptosis[23-25]. This confers an increased resistance to apoptosis and a propensity to leukemic cell proliferation. Low levels of miR-15 or miR-16 are observed in patients with monoallelic deletions and in many patients without

del(13)(q14) (ref. 15, 21, 22, 26-28). Additional support for the role of the miR-15/miR-16 locus in CLL pathogenesis comes from the New Zealand Black (NZB) mice strain harboring a germ-line point mutation downstream of the miR-16 locus, which prevents normal expression of both miR-15 and miR-16 and facilitates leukemia onset and possibly autoimmune manifestations[29]. An analogous lesion, present in particular families, genetically predisposes humans to CLL and possibly to other neoplasias[30]. Finally, the selective deletion of the miR-15/miR-16 locus in mice predisposes the development of a CLL-like leukemia[16, 31]. Therefore, impairment of miR-15 and miR-16 function may be involved in promoting the initial phases of leukemogenesis; however, little is known regarding the role of these lesions in maintaining the transformed status and the clonal expansion of full-blown leukemia[32].

Here, we investigated the possibility of interfering with both miR-15 and miR-16 expression by CLL cells, both in *in vivo* and *in vitro*.

Materials and Methods

Patients and CLL cell preparations.

Newly diagnosed CLL patients from participating Institutions were enrolled within 12 months from diagnosis in the O-CLL1 protocol (clinicaltrial.gov identifier NCT00917540). All participants provided written informed consent in accordance with the declaration of Helsinki and the study was approved by the appropriate institutional review boards. Supplementary Table S1 summarizes the phenotype and the major cytogenetic features of CLL cases (n=59) selected for *in vitro* (n=48) and *in vivo* (n=17) experiments reported in this study[11, 33, 34].

PBMCs from patients with CLL were isolated by Ficoll-Hypaque (Seromed, Biochrom) density gradient centrifugation. In selected experiments, CD19-positive CLL cells were enriched by negative selection with the EasySep-Human B-cell Enrichment Kit without CD43 depletion (STEMCELL Technologies, Voden Medical Instruments S.p.A).

Cell transfection

MirVana™ miRNA mimics or inhibitors (Ambion Inc, Thermo Fisher Scientific, Grand Island, NY, USA) were delivered to CLL cells with a Neon Transfection System (Invitrogen, Thermo Fisher Scientific) at the final concentration of 50 nM/2×10^6 CLL cells. Optimal transfection and survival of CLL cells was obtained by applying 1 pulse at 2150 pulse voltage and 20 pulse width, as indicated by the manufacturer for the primary blood-derived suspension cells protocol. After transfection, cell suspensions were seeded in 24-well plates containing 500 µL of culture medium without antibiotics [RPMI-1640 with L-glutamine and 10% FBS (Gibco, Thermo Fisher Scientific), Sodium piruvate 0.1% (Euroclone)] at 37°C and incubated at the final

concentration of 2×10^6 CLL cells/mL/well in a 5% CO2 atmosphere. The following miRNA mimics and inhibitors were employed: hsa-miR-15a-5p, hsa-miR-16-5p, and miRNA Negative Control (CTR)#1, miRNA Inhibitor Negative CTR #1.

Evaluation of miRNA expression

MiR-15 and miR-16 expression was evaluated with two methods: SmartFlare RNA Detection Probes (Merck Millipore, France) in n=13 CLL cases and quantitative real time PCR (q-RT PCR) (n=38 CLL cases), Supplementary materials and methods and Figure S2).

SmartFlare technology is useful to study miRNA expression at the single-cell level. SmartFlare™ RNA Detection Probes, are constituted by tiny gold nanoparticles conjugated to oligonucleotides duplexed with reporter strands (oligo+fluorophore). When Smartflare probes bind to their complementary RNA sequences the fluorophore is released and can be detected by flow-cytometry (FC). The following Smartflare probes conjugated with the Cyanine 5 (Cy5) fluorophore were used: SF-430/ miR-15a-5p (miR-15 CY5); SF-178/ miR-16-5p (miR-16 CY5); SF-102 /Scramble CTR Cy5. The latter reagent does not bind to any RNA sequences within the cells and is used to measure the level of background fluorescence within CLL cells. Cells were incubated with Smartflare probes overnight, harvested and analyzed by FACSCanto (BD Biosciences) and DIVA 6 (BD Biosciences) or FLOWJO V.9.8.3 software (Treestar Inc.).

Counterstaining with propidium iodide (PI; 50 mg/mL, Sigma) in isotonic solution was employed to evaluate cell viability.

Changes in miR-15/miR-16 expression following transfection with miRNA mimics or inhibitors were expressed as:

% fold induction= (%smartflare positive cells transfected with miR-15/miR-16 mimic) - (%smartflare positive cells transfected with miR-CTR mimic) / (%smartflare positive cells transfected with miR-15/miR-16 mimic)*100

% fold inhibition= (%smartflare positive cells transfected with miR-CTR inhibitor) - (%smartflare positive cells transfected with miR-15/miR-16 inhibitor) / (%smartflare positive cells transfected with miR-CTR inhibitor) *100

Apoptosis assays

Cultured cells were double stained with Annexin V-FITC conjugate (cat. 556419, BD Biosciences Pharmingen, San Josè, CA, USA), and PI in isotonic solution, and then analyzed by FC. Viable cells were defined as double negative cells[35].

Xenogeneic mouse transplantation

Six to eight week old female NOD/Shi-scid,γcnull (NSG) mice (The Jackson Laboratory), a xenograft model for CLL growth in vivo[36, 37] were housed in sterile enclosures under specific pathogen-free conditions. All procedures involving animals were performed in the respect of the current National and International regulations and were reviewed and approved by the Licensing and Animal Welfare Body of the IRCCS-AOU San Martino-IST National Cancer Research Institute, Genoa, Italy.

Depending on the number of leukemic cells available for animal injection, groups of 2-3 NSG mice were employed for each test and treatment group. The number of animals used for each treatment is detailed in brackets in Table 1 and Supplementary Tables S3-S5. Full details are in Supplementary Material and Methods.

In miRNA pre-treatment experiments NSG mice (n= 38) were inoculated with CLL cells (n=6) transfected with miRNA mimic/inhibitors and cultured for 6 h prior to injection. A total of $50x10^6$ CLL cells per mouse were injected together with a proportion of autologous T cells (approximately 5-10%).

After four weeks, mice were anesthetized by intraperitoneal injection of combination of xylazine (10 mg/kg) and ketamine (100 mg/kg) and analyzed by Magnetic Resonance Imaging (MRI) with USPIO contrast reagent[38].

On termination of the experiment (maximum 6 weeks from start), animals were sacrificed in a saturated CO2 chamber and autopsies were performed. Spleens were evaluated by FC and by immunohistochemical (IHC) analysis. The Animal Welfare Body posed a time limit to the experimental protocol to prevent unneeded suffering.

Fresh spleen samples were enzymatically digested using the Spleen Dissociation Kit (Miltenyi Biotec) and mechanically resuspended with gentleMACS™ Dissociator (Miltenyi Biotec). The single-cell suspensions were stained with anti-human CD45-FITC (555482), CD19-PECy7(557835), CD5-APC(555355), (BD Biosciences) and analyzed by FC. Apoptosis was evaluated using Annexin-V-FITC, CD19-PE-Cy7, CD5-PE (555353) (BD Biosciences), CD45-APC(130-091-230, Miltenyi Biotec,) cell staining.

Formalin-fixed and paraffin-embedded spleen specimens were analyzed for the presence of human CLL infiltrates and for the presence of co-injected bystander T-cells by IHC as detailed above[38]. The primary antibodies anti-CD20 Mouse monoclonal antibody (760-2531, clone L26- Ventana Medical System, Roche) and CD3 Rabbit Monoclonal Antibody (790-4341, clone 2GV6- Ventana Medical System, Roche) were incubated for 30 min at 37°C and signals

revealed using the polymeric detection system, Ultraview Universal Red Detection Kit (Ventana Medical System). An appropriate positive tissue control was used for each staining run; the negative control consisted of performing the entire IHC procedure on adjacent sections in the absence of the primary antibody; the sections were counter-stained (automatically) with Gill's modified hematoxylin and then cover-slipped. The sections were evaluated by two observers with an Olympus light microscope using 4X, 10X, 40X and objectives under a Leica DMD108 optical digital microscope (Leica Microsystems).

To evaluate therapeutic effects of miRNA, CLL (n=11) engraftment in the spleen was determined by MRI following USPIO contrast reagent injection after 2-3 weeks from cell injection. At this stage, mice were treated intraperitoneally [every second day with mirVana™ miRNA mimic, (In Vivo Ready formulation, Ambion Inc)] complexed with Invivofectamine 2.0 (Thermo Fisher Scientific) at a final concentration of 0.7 mg/mL (200 μL/mouse). Overall three doses were administered. The following miRNA were used: hsa-miR-15a-5p, hsa-miR-16-5p, miRNA negative control#1. Three days from the last injection, mice (n=74) were analyzed again by MRI and then sacrificed in a saturated CO2 chamber and autopsies were performed. Spleens were analyzed by FC and IHC. Apoptosis was evaluated by Annexin-V-FITC, CD19-PE-Cy7, CD5-PE, CD45-APC, and FC or by Cleaved Caspase-3 (Asp175) (5A1E) Rabbit mAb (9664, Cell Signaling Technology, Danvers, MA, USA) and IHC on spleen tissue sections.

Magnetic Resonance Imaging

All *in-vivo* MRI experiments and MRI analyses, using USPIO nanoparticles, were carried out and acquired as previously described[38]. Details are reported in the Supplementary Information.

205 ***Definition of IHC index***

206 The IHC index is a measure of the spread of leukemia based on the average diameters of
207 the follicular lesions. We assigned a numerical value of 1 to the follicles with diameters±s.d. of
208 102(±90) x 42(±7) μm; a value of 3 to follicles with a diameter 195(±80) x 138(±85) μm; a value
209 of 6 to follicles between 399(±245) x 300(±39), and a value of 12 to follicles between 734(±461)
210 x 540(±167). The IHC index is given by the sum of the number of follicles multiplied by the
211 value assigned according to size (Supplementary Figure S3).

212

213 ***Statistical analysis***

214 The statistical package SPSS for Windows, v13.0, 2004 software (SPSS UK) was used
215 for all analyses of statistical significance from adequately powered sample sizes for two-tailed
216 tests. Statistical comparisons between related samples were carried out by nonparametric
217 Wilcoxon signed rank (paired data) or by Mann-Whitney U (unpaired data) tests. A value of
218 $P<0.05$ was considered significant for all statistical calculations. Values are given as
219 mean±s.e.m. or mean±s.d. as stated in figure legends, which was calculated invariably from n
220 (the number of patients or animals, biological replicates). All exact P-values are provided in the
221 figure panels, in figure legends or in Results section.

Results

Transfection of miR-15 and miR-16 mimics or inhibitors into CLL cells in vitro

Transfection of miRNAs mimics or inhibitors into purified CLL cells was verified by FC using Smartflare technology and qRT-PCR.

For the experiments with miRNA mimics, 7 CLL cases with biallelic del(13)(q14) deletions were selected (Supplementary Information and Table S1 for case characteristics). At 24-h after transfection, a significantly larger number of cells were found to express miR-15 (%fold induction=79±5, mean±s.e.m.) and miR-16 (%fold induction=75±5) compared to control preparations (P=0.015) (Figure 1a and Supplementary Figure S4a). Comparable data were obtained by qRT-PCR (Supplementary Figure S2a).

For experiments with miRNA inhibitors, we selected 6 CLL cases that did not display biallelic del(13)(q14) and expressed miR-15 and miR-16 to a variable extent. Transfection with specific miRNA inhibitors efficiently reduced miRNA expression in all CLL clones compared to controls (%fold inhibition=54±4, mean±s.e.m., for miR-15; and %fold inhibition=59±4 for miR-16) (P=0.03) (Figure 1c and Supplementary Figure S4b). Again, comparable data were obtained when miRNA expression was measured by qRT-PCR (Supplementary Figure S2b).

Since miR-15 and miR-16 expression may impact on CLL cell survival *in vitro*, purified cells from 12 CLL cases with biallelic del(13)(q14) were transfected with miR-15 or miR-16 miRNA mimics and cultured for up to 72 h. Viable cells were measured at different time intervals (Supplementary Figure S5a shows the data of a representative experiment). A significant decrease in cell viability (%fold reduction mean±s.e.m.=53±7 and 48±6 for miR-15 and miR-16 mimics, respectively in 11/12 CLL samples) after 48 h (P=0.001 for miR-15 and

P=0.0015 for miR-16) was observed. Figure 1b shows the pooled data from the tests performed while experiments on individual CLL cases are reported in Supplementary Figure S6a. Viability of cells from the CLL case CG0620, carrying a *TP53* mutation, did not change, but the cells from two other CLL cases (MG0248, PA0254), also displaying *TP53* mutations, showed a substantial drop in cell viability following transfection with either miR-15 or miR-16 (Supplementary Table S1 and Figure S6a).

Co-transfection of biallelic del(13)(q14) CLL cells with both miR-15 and miR-16 miRNAs never resulted in an additive/synergistic effect (data not shown). Consistent with previous observations, transfection of miR-15 or miR-16 into del(13)(q14) CLL cells caused down-regulation of BCL2 or MCL1 (antiapoptotic) and of Cyclin D1 or D2 (cell cycle induction) proteins encoded by target genes of these miRNAs[23, 24]. In contrast, Survivin, which is involved in an alternative apoptotic pathway, was not down-regulated (Supplementary Figure S6b-c).

Inhibition of miR-15 or miR-16 expression with specific miRNA inhibitors resulted in a substantial increase in CLL cell viability. Supplementary Figure 5b reports the cell viability of a representative CLL case. A significant increase in cell viability was measured until 48-hours culture, whereas at 72 hours, a drop in cell viability was observed both in the presence of miR-15/miR-16 inhibitors and in the presence of miR-CTR inhibitor, although there were still differences in the two conditions. Pooled viability data, measured after a 48-h culture from a group of 24 CLL cases displaying different cytogenetic features (Supplementary Table S2 and Supplementary Figure S7), are summarized in Figure 1d (%fold increase=40±3 and 42±4 with miR-15 or miR-16 inhibitor, respectively; $P<0.0001$) and show that miRNA inhibition expression resulted consistently in a better in vitro survival of CLL cells.

Effects of in vitro transfection with miRNA-15 or miRNA-16 mimics/inhibitors on the growth of CLL cells in NSG mice

Purified cells from four CLL cases with biallelic del(13)(q14) were transfected with miR-15, miR-16 or miR-CTR mimics, cultured for 6-h and then injected intravenously (i.v.) into NSG mice together with autologous T cells (B/T cell ratio 5-10:1). Two/three mice were used for each treatment group. Disease engraftment was measured after 4 weeks by USPIO-MRI of the spleen[38]. Iron uptake is inversely correlated with the presence of CLL follicles-like structures which prevent iron uptake. Signal-to-Noise ratio change (ΔSNR%) values are higher when low iron levels enter the splenic tissue. Thus, higher uptake of the USPIO contrast reagent was observed in the spleens of NSG mice receiving CLL cells transfected with miR-15 or miR-16 mimics which resulted into a lower ΔSNR% value compared to the spleens of mice receiving miR-CTR-transfected CLL cells (Figure 2a). The ΔSNR% of mice injected with miR-15 (mean±s.d.= −31.1±25.1) or miR-16 (mean±s.d.= −18.2±28.19) mimics pre-treated cells res.e.m.bled that of NSG mice that had not received leukemic cells (mean±s.d..= −54.3±15), whereas this value was higher (+30.7±23.4) in the mice receiving miR-CTR pre-treated cells. ΔSNR% values of mice groups pre-treated with miR-15 (n=7) or with miR-16 (n=6) were significantly lower compared to those pre-treated with miR-CTR (n=8) (P=0.001 for miR-15; P=0.01 for miR-16). This MRI pattern was likely related to the lower number of neoplastic foci within the splenic white pulp, a finding consistent with the observation of a lower number of follicle-like structures detected by IHC with anti-CD20 mAb in the spleen of mice receiving miR15/16 treated cells compared to controls. Likewise, the IHC index (as detailed in Supplementary Figure S3) of mice receiving CLL cells treated with miR-15/16 mimics was decreased compared to that of mice receiving cells transfected with miR-CTR. The average ±s.d.

290 of the IHC index reduction was 68±11 and 67±11 following transfection of miR-15 and miR-16
291 mimics, respectively (Figure 2c) (P=0.0078 for both miRNAs compared to miR-CTR). FC
292 showed a significantly lower proportion of CD19+CD5+ cells in the spleens of mice inoculated
293 with miR-15/16-mimic-transfected CLL cells than in controls (P=0.012) (Figure 2e and
294 supplementary Figure S8a). B cells recovered from NSG mice consistently shared the same BCR
295 gene rearrangements as the leukemic clone used for injection, whereas T cells displayed
296 oligoclonal TCR rearrangments (data not shown).

297 Cells from two CLL cases (PM0608, PA0145) lacking del(13)(q14) were pre-treated with
298 miR-15 or miR-16 inhibitors *in vitro* and subsequently injected into NSG mice together with T
299 cells according to the same schedule described above. This treatment resulted in a better splenic
300 engraftment of the CLL cells as documented by the differences in the ΔSNR% (Figure 2b). In the
301 spleen of mice injected with the cells from PM608 CLL case, these values were of +49±8.4 and
302 +33±19.3 after pre-treatment of the cells with miR-15 and miR-16 inhibitors, respectively and of
303 +8±11.1 after cell pretreatment with miR-CTR inhibitors. This was paralleled by an average IHC
304 index increase (mean±s.d..) of 69±6% and 71±17% respectively, in mice inoculated with miR-15
305 or miR-16 inhibitor pre-treated cells (P=0.039 for miR-15 and P=0.05 for miR-16 inhibitors
306 compared to miR-CTR inhibitor, Figure 2d). Consistent with these data was the significant
307 increase in the percentage of CD45+CD19+CD5+ cells observed by FC in the mice inoculated
308 with miRNA-inhibitor-treated cells (71±3% and 69±1%, mean±s.d., respectively) (Figure 2f, and
309 supplementary Figure S8b). All data are detailed in Supplementary Table S3. Again, the BCR
310 and TCR gene rearrangement analyses confirmed that the engrafted B cells were mostly from the
311 leukemic clones, whereas T cells were oligoclonal (not shown).
312

Inhibition of CLL cell expansion in NSG mice by treatment with miR-15 and miR-16 mimics.

Next, we investigated whether administration of miRNA mimics could inhibit the expansion of a previously inoculated CLL clone in NSG mice. In preliminary tests, six NSG mice were injected with MG0248 CLL cells. After four weeks, a single potentially therapeutic dose of miR-15 miR-16 or miR-CTR complexed with Invivofectamine was administered intraperitoneally. Mice were sacrificed 24-h after miRNA administration and CLL cells (CD45+, CD19+ and CD5+) were purified by FACS sorting from splenic cell suspensions (the resulting preparations contained >98% CLL cells). qRT-PCR analysis showed an increase of miR-15 (fold increase=407.80) and of miR-16 (fold increase 34.15) levels above control mice injected with miR-CTR (Supplementary Figure S9).

Next, CLL cells from six cases with biallelic del(13)(q14) were inoculated into NSG mice together with T cells (NSG-CLL) and CLL engraftment was verified in the spleen after approximately two weeks by MRI[38]. Mice found to have an above-average splenic ΔSNR%, compared to NSG mice that had not received leukemic cells (NSG-CTR, n=12, ΔSNR% −54.3±15, mean±s.d.), were placed on treatment with miR-15 or miR-16 mimics or miR-CTR (one injection on alternate days for a total of three injections). Three days after the final treatment, splenic infiltration by leukemic cells was evaluated (Figure 3 and 4). On MRI (exemplified in Figure 3a and 3b), miR-CTR treated mice displayed a splenic infiltration by leukemic cells with an 63±14 average increase of ΔSNR% over that of mice not receiving leukemic cells ($p < 0.0001$). In contrast, mice treated with miR-15 or miR-16 mimics showed a significant ΔSNR% decrease ($P<0.0001$ and $P=0.0002$, respectively) compared to mice before therapy administration (Figure 3c). The values of the treated mice were similar to those of NSG-CTR mice not receiving CLL cell inocula. The ΔSNR% values of mice treated with miR-CTR

following CLL cell inoculation were similar to or greater than those at therapy start time point (P=0.002) (Figure 3c). These results predicted a response to therapy, which was subsequently confirmed by FC analysis [average percentage CLL cells reduction of 61±8 (P=0.0006) and of 75±12 (P=0.0001) after miR-15 and miR-16 mimics treatment, respectively *versus* mice treated with miR-CTR] (Fig 3d) and IHC. A significantly lower IHC index was observed in mice treated with miR-15 or miR-16 compared to mice treated with miR-CTR [(average IHC index reduction 62±15 (P=0.0007) and 78±22 (P=0.02), respectively] (Figure 3e and Supplementary Table S4).

IHC analysis showed an almost complete disappearance of the typical aggregates of leukemic (CD20+) cells after treatment with miR-15 or miR-16 mimics (Figure 4a and Supplementary Figure S3b). However, autologous T cells (CD3+ cells), surrounding what was presumably the area of the previously existing CLL cell aggregates/nodules, were still present in a substantial number, possibly indicating that T cells were not affected by treatment (Figure 4b). Cleaved CASP3 could be observed in the "empty nodules" possibly indicating apoptotic leukemic cells (Figure 4c and Supplementary Figure S10) as also suggested by the observation of an increased percentage of Annexin V positive CLL cells (P<0.0001) in the splenic cell suspension by FC (Figure 4d and Supplementary Table S5).

Decrease *in vitro* viability and growth ability of CLL cells with different cytogenetic features following transfection with miR-15 or miR-16 mimics

We extended our observations to a set of 26 CLL cases lacking biallelic del(13)(q14) (Figure 5 and Supplementary Table S1). The cells from these cases, which expressed different levels of miR-15 and miR-16 as evaluated by qRT-PCR (Supplementary Figure S1c,d), were purified and transfected with miR-15, miR-16 mimics or miR-CTR (Supplementary Figure S2c).

Cell viability was significantly decreased following transfection in most cases ($P<0.001$, Figure 5a, b). Decreased cell viability also was observed when the two major CLL groups were analyzed separately: i.e. those with monoallelic del(13)(q14) [statistically significant differences in the miR-15-mimic ($P=0.01$), miR-16-mimic ($P=0.005$) treated cells compared to controls] and the group with normal FISH ($P=0.004$).

In addition, viability of the cells from other cases, including one with del(11)(q22.3), involving the ATM gene, and others with p53 mutations or del(17)(p13.1) was reduced following miR-15 and miR-16 mimic transfection .

Finally, NSG mice were engrafted with cells from two cases harboring monoallelic del(13)(q14) (FP0499, GN0095), one case with trisomy 12 (RD0468), one with a normal FISH pattern (VS0624) and one with del(17)(p13.1) and a *TP53* mutation on the remaining allele (RM0626), and were subsequently treated with miR-15 or miR-16 as above. A significant reduction of splenic disease was observed by FC ($P=0.0001$ and $P=0.006$ following miR-15 or miR-16 mimic treatment, respectively compared to miR-CTR) (Table 1). A decrease in the IHC index of 72±18% and 74±10% following treatment with miR-15 and miR-16 mimics, respectively ($P=0.001$) was observed in four of the CLL cases tested. Case RM0626 represented a remarkable exception since treatment with the miRNA mimics consistently failed to significantly block the growth of CLL cells *in vivo*. Of note is the finding that this case had low miR-15 and medium to high miR-16 expression. Thus, the findings were unlikely related to the possibility that the miRNA values were already so high that could not be changed by the transfection. Rather, a completely dysfunctional *TP53* was the possible cause for the findings.

Discussion

This study demonstrates that *in vitro* transfection of miR-15 and miR-16 mimics into CLL cells with del(13)(q14) results in a significant inhibition of their subsequent growth in NSG mice. Furthermore, administration of miR-15 or miR-16 mimics to NSG mice, in which these CLL cells were already engrafted and proliferating, caused significant tumor regression. Both observations are in line with the notion that miR-15 and miR-16 control the cell apoptotic apparatus and proliferative capacities[17, 23, 24]. No additive/synergistic effects were noted when miR-15 and miR-16 mimics were co-transfected, suggesting that the regulatory controls of the two miRNAs on the expression of other genes largely overlap, a consideration consistent with the notion that miR-15 and miR-16 interact with the same 3'-UTR region of BCL-2 mRNA[24].

Selective inhibition of miR-15 and miR-16 expression in CLL cells resulted in improved *in vitro* survival and a more robust expansion in NSG mice[16]. In contrast, enforced expression of miR-15 or miR-16 in cells retaining the capacity to express these miRNAs resulted in impaired *in vitro* survival or diminished expansion in NSG mice. Both findings provide further support for the regulatory role of intracellular miR-15/miR-16 concentrations in full-blown CLL [14, 23, 24, 32] (Figure 5). The experimental design utilized here was intended to obtain a specific and selective inhibition or replacement of miR-15 and miR-16 without further influence of other gene segments such as *Dleu2* or *Dleu7* (ref. 39), the absence of which have been shown to synergize with that of miR-15 and miR-16 in CLL pathogenesis. Thus, the data demonstrate that low/absent expression of miR-15 and miR-16 plays a crucial pathogenetic role *per sè,* in line with the observation that replacement of these miRNAs in NZB mice using suitable viral carriers blocks the expansion of CLL-like cells both *in vivo* and *in vitro*[40].

MiR-15 or miR-16 mimics did not apparently interfere with the function of T cells that are normally needed to support *in vivo* CLL cell growth. In the experiments where CLL cell growth in NSG mice was inhibited by pre-exposure to miR-15/miR-16 mimics *in vitro* (see Figure 2), the T cells were added to the purified CLL cells following their *in vitro* exposure to these miRNAs. However, in experiments, where transfection was carried out *in vitro* on unfractionated cell suspensions, containing both T and CLL cells, before injection into mice, we observed an unaltered distribution pattern of T cells in the spleen of mice even in the presence a largely diminished proportion of B cells. Moreover, when mice were treated with miR-15 or miR-16 mimics *in vivo*, seemingly unaltered T cell proportions were observed surrounding the "empty" areas, previously occupied by CLL cells (Figure 4). Thus, inhibition of CLL cell growth in NSG mice presumably occurred through interference of the transfected mimics with the CLL cell survival/proliferating apparatus, rather than through an indirect action on the T cells promoting CLL cell growth. Whether or not progressive CLL cell death, induced by the transfected miRNA mimics *in vivo*, may lead to T cell immune-priming capable of causing further CLL cell elimination is presently unknown.

A final issue concerns the potential use of miR-15 and miR-16 for therapy. MiRNA mimics are effective on CLL cells growing *in vivo* and on CLL cells with additional chromosomal alterations; however, some results from both *in vivo* and *in vitro* experiments showed that the presence of *TP53* gene mutations/deletions may render administration of the miR-15 and miR-16 mimics ineffective. This is expected, given the close interactions between miR-15 and miR-16, *TP53* and the cluster of miR-34 genes in the regulation of cell survival/apoptosis[41, 42]. Nevertheless, not all cases with *TP53* defects failed to respond to miRNA mimics treatment suggesting heterogeneity of functional TP53 alterations. These observations

425 are being extended to additional cohorts of patients including more advanced stage/relapsed
426 patients that more frequently harbor additional *TP53* alterations[43-46].

427 We provide proof of principle data supporting the potential use of miRNA mimics to
428 block CLL clonal expansion. Additional miRNAs, other than miR-15 or miR-16, may become
429 suitable therapeutic targets, since a number of studies have demonstrated anomalous expression
430 of various miRNAs in CLL cells compared to normal cells[11, 22, 30]. Moreover, when certain
431 miRNA are overexpressed, they can be targeted by miRNA inhibitors[47]. Several anomalies in
432 miRNA expression have prognostic/predictive value for disease course and outcome, indicating a
433 potential mechanistic role in the disease pathogenesis/progression[22-24, 30, 48-52]. Thus, the miRNA
434 approach, especially if multiple miRNA mimics and inhibitors can be targeted, either alone or in
435 combination with other drugs, may represent an additional therapeutical strategy. In connection
436 with this, it should be noted that therapy with miR inhibition/replacement is being employed in a
437 variety of experimental tumors. Moreover, there are many available studies on human tumors,
438 some of which have reached the clinical stage I, with potentially promising results[53]. Thus, miR
439 therapy may represent a "real" tool in the future armamentarium of drugs usable in CLL, a
440 disease that so far has escaped attempts towards a radical cure.

Acknowledgments: In addition to the Authors listed, the following investigators participated in this study as part of the GISL - Gruppo Italiano Studio Linfomi: Gianni Quintana, Divisione di Ematologia, Presidio Ospedaliero "A.Perrino", Brindisi; Giovanni Bertoldero, Dipartimento di Oncologia, Ospedale Civile, Noale, Venezia; Paolo Di Tonno, Dipartimento di Ematologia, Venere, Bari; Robin Foà and Francesca R Mauro, Divisione di Ematologia, Università La Sapienza, Roma; Nicola Di Renzo, Unità di Ematologia, Ospedale Vito Fazzi, Lecce; Maria Cristina Cox, Ematologia, A.O. Sant'Andrea, Università La Sapienza, Roma;Stefano Molica, Dipartimento di Oncologia ed Ematologia, Pugliese-Ciaccio Hospital, Catanzaro; Attilio Guarini, Unità di Ematologia e Trapianto di Cellule Staminali, Istituto di Oncologia "Giovanni Paolo II", Bari; Antonio Abbadessa, U.O.C. di Oncoematologia Ospedale "S. Anna e S. Sebastiano", Caserta; Francesco Iuliano, U.O.C. di Oncologia, Ospedale Giannettasio, Rossano Calabro, Cosenza; Omar Racchi, Ospedale Villa Scassi Sampierdarena, Genova; Mauro Spriano, Ematologia, A.O. San Martino, Genova; Felicetto Ferrara, Divisione di Ematologia, Ospedale Cardarelli, Napoli; Monica Crugnola, Ematologia, CTMO, Azienda Ospedaliera Universitaria di Parma; Alessandro Andriani, Dipartimento di Ematologia, Ospedale Nuovo Regina Margherita, Roma; Nicola Cascavilla, Unità di Ematologia e Trapianto di Cellule Staminali, IRCCS Ospedale Casa Sollievo della Sofferenza, San Giovanni Rotondo; Lucia Ciuffreda, Unità di Ematologia, Ospedale San Nicola Pellegrino, Trani; Graziella Pinotti, U.O. Oncologia Medica, Ospedale di Circolo Fondazione Macchi, Varese; Anna Pascarella, Unità Operativa di Ematologia, Ospedale dell'Angelo, Venezia-Mestre; Maria Grazia Lipari, Divisione di Ematologia, Ospedale Policlinico, Palermo, Francesco Merli, Unità Operativa di Ematologia, A.O.S. Maria Nuova, Reggio Emilia; Luca Baldini Istituto di Ricovero e Cura a Carattere Scientifico Cà Granda-Maggiore Policlinico, Milano; Caterina Musolino, Divisione di Ematologia, Università di Messina; Agostino Cortelezzi, Ematologia and CTMO, Foundation IRCCS Ca' Granda Ospedale Maggiore Policlinico, Milano; Francesco Angrilli, Dipartimento di Ematologia, Ospedale Santo Spirito, Pescara; Ugo Consoli, U.O.S. di Emato-Oncologia, Ospedale Garibaldi-Nesima, Catania; Gianluca Festini, Centro di Riferimento Ematologico-Seconda Medicina, Azienda Ospedaliero-Universitaria, Ospedali Riuniti, Trieste; Giuseppe Longo, Unità di Ematologia, Ospedale San Vincenzo, Taormina; Daniele Vallisa and Annalisa Arcari, Unità di Ematologia, Dipartimento di Onco-Ematologia, Guglielmo da Saliceto Hospital, Piacenza; Francesco Di Raimondo and Annalisa Chiarenza, Divisione di Ematologia, Università di Catania Ospedale Ferrarotto, Catania; Iolanda Vincelli, Unità di Ematologia, A.O. of Reggio Calabria; Donato Mannina, Divisione di Ematologia, Ospedale Papardo, Messina, Italy.

Funding: This work was supported by: Associazione Italiana Ricerca sul Cancro (AIRC) Grant 5 x mille n.9980, (to M.F., F.M. A. N., P.T. and M.N.) ; AIRC I.G. n. 14326 (to M.F.), n.10136 and 16722 (A.N.), n.15426 (to F.F.). AIRC and Fondazione CaRiCal co-financed Multi Unit Regional Grant 2014 n.16695 (to F.M.). Italian Ministry of Health 5x1000 funds (to S.Z. and F.F). A.G R. was supported by Associazione Italiana contro le Leucemie-Linfomi-Mielomi (AIL) Cosenza - Fondazione Amelia Scorza (FAS). S.M. C.M., M.C., L.E., S.B. were supported by AIRC.

Author contributions: Conception and design: G.C., G.B., F.F., M.F.; Development of methodology: G.C., S.M., C.M., G.B, M.C., D.R, R.M., S.S., S.B., L.E, S.F; Acquisition of data: G.C., S.M., L.E., M.C., G.B., M.M., S.F., S.S., D.R, R.M., F.V., S.Z., F.M., M.N.; Analysis and interpretation of data : G.C., S.M., G.B., C.M, A.N., S.S., M.C., S.F, C.E.N, M.C., F.R, L.B,

F.F., S.Z., M.N., P.T., M.G., M.T., M.F., F.M.; Writing, review, and/or revision of the manuscript: G.C, A.G.R., M.N., P.T., A.N., F.F., M.F.; Study supervision: G.C., F.F, M.F. All authors reviewed and approved the manuscript.

Supplementary information is available at Leukemia website (http://www.nature.com/leu)

References

1. Chiorazzi N, Rai KR, Ferrarini M. Chronic lymphocytic leukemia. *N Engl J Med* 2005; **352**(8)**:** 804-815.

2. Dohner H, Stilgenbauer S, James MR, Benner A, Weilguni T, Bentz M*, et al.* 11q deletions identify a new subset of B-cell chronic lymphocytic leukemia characterized by extensive nodal involvement and inferior prognosis. *Blood* 1997; **89**(7)**:** 2516-2522.

3. Neilson JR, Auer R, White D, Bienz N, Waters JJ, Whittaker JA*, et al.* Deletions at 11q identify a subset of patients with typical CLL who show consistent disease progression and reduced survival. *Leukemia* 1997; **11**(11)**:** 1929-1932.

4. Dohner H, Stilgenbauer S, Benner A, Leupolt E, Krober A, Bullinger L*, et al.* Genomic aberrations and survival in chronic lymphocytic leukemia. *N Engl J Med* 2000; **343**(26)**:** 1910-1916.

5. Grever MR, Lucas DM, Dewald GW, Neuberg DS, Reed JC, Kitada S*, et al.* Comprehensive assessment of genetic and molecular features predicting outcome in

patients with chronic lymphocytic leukemia: results from the US Intergroup Phase III Trial E2997. *J Clin Oncol* 2007; **25**(7)**:** 799-804.

6. Stilgenbauer S, Zenz T, Winkler D, Buhler A, Schlenk RF, Groner S*, et al.* Subcutaneous alemtuzumab in fludarabine-refractory chronic lymphocytic leukemia: clinical results and prognostic marker analyses from the CLL2H study of the German Chronic Lymphocytic Leukemia Study Group. *J Clin Oncol* 2009; **27**(24)**:** 3994-4001.

7. Fischer K, Cramer P, Busch R, Bottcher S, Bahlo J, Schubert J*, et al.* Bendamustine in combination with rituximab for previously untreated patients with chronic lymphocytic leukemia: a multicenter phase II trial of the German Chronic Lymphocytic Leukemia Study Group. *J Clin Oncol* 2012; **30**(26)**:** 3209-3216.

8. Zenz T, Habe S, Denzel T, Mohr J, Winkler D, Buhler A*, et al.* Detailed analysis of p53 pathway defects in fludarabine-refractory chronic lymphocytic leukemia (CLL): dissecting the contribution of 17p deletion, TP53 mutation, p53-p21 dysfunction, and miR34a in a prospective clinical trial. *Blood* 2009; **114**(13)**:** 2589-2597.

9. Kalachikov S, Migliazza A, Cayanis E, Fracchiolla NS, Bonaldo MF, Lawton L*, et al.* Cloning and gene mapping of the chromosome 13q14 region deleted in chronic lymphocytic leukemia. *Genomics* 1997; **42**(3)**:** 369-377.

10. Rawstron AC, Bennett FL, O'Connor SJ, Kwok M, Fenton JA, Plummer M*, et al.* Monoclonal B-cell lymphocytosis and chronic lymphocytic leukemia. *N Engl J Med* 2008; **359**(6)**:** 575-583.

11. Morabito F, Mosca L, Cutrona G, Agnelli L, Tuana G, Ferracin M*, et al.* Clinical monoclonal B lymphocytosis versus Rai 0 chronic lymphocytic leukemia: A comparison of cellular, cytogenetic, molecular, and clinical features. *Clin Cancer Res* 2013; **19**(21)**:** 5890-5900.

12. Liu Y, Corcoran M, Rasool O, Ivanova G, Ibbotson R, Grander D*, et al.* Cloning of two candidate tumor suppressor genes within a 10 kb region on chromosome 13q14, frequently deleted in chronic lymphocytic leukemia. *Oncogene* 1997; **15**(20)**:** 2463-2473.

13. Migliazza A, Bosch F, Komatsu H, Cayanis E, Martinotti S, Toniato E*, et al.* Nucleotide sequence, transcription map, and mutation analysis of the 13q14 chromosomal region deleted in B-cell chronic lymphocytic leukemia. *Blood* 2001; **97**(7)**:** 2098-2104.

14. Calin GA, Dumitru CD, Shimizu M, Bichi R, Zupo S, Noch E*, et al.* Frequent deletions and down-regulation of micro- RNA genes miR15 and miR16 at 13q14 in chronic lymphocytic leukemia. *Proc Natl Acad Sci U S A* 2002; **99**(24)**:** 15524-15529.

15. Mosca L, Fabris S, Lionetti M, Todoerti K, Agnelli L, Morabito F, *et al.* Integrative genomics analyses reveal molecularly distinct subgroups of B-cell chronic lymphocytic leukemia patients with 13q14 deletion. *Clin Cancer Res* 2010; **16**(23)**:** 5641-5653.

16. Klein U, Lia M, Crespo M, Siegel R, Shen Q, Mo T, *et al.* The DLEU2/miR-15a/16-1 cluster controls B cell proliferation and its deletion leads to chronic lymphocytic leukemia. *Cancer Cell* 2010; **17**(1)**:** 28-40.

17. Sellmann L, Scholtysik R, Kreuz M, Cyrull S, Tiacci E, Stanelle J, *et al.* Gene dosage effects in chronic lymphocytic leukemia. *Cancer Genet Cytogenet* 2010; **203**(2)**:** 149-160.

18. Lagos-Quintana M, Rauhut R, Lendeckel W, Tuschl T. Identification of novel genes coding for small expressed RNAs. *Science* 2001; **294**(5543)**:** 853-858.

19. Ghildiyal M, Zamore PD. Small silencing RNAs: an expanding universe. *Nat Rev Genet* 2009; **10**(2)**:** 94-108.

20. Hausser J, Zavolan M. Identification and consequences of miRNA-target interactions--beyond repression of gene expression. *Nat Rev Genet* 2014; **15**(9)**:** 599-612.

21. Ouillette P, Erba H, Kujawski L, Kaminski M, Shedden K, Malek SN. Integrated genomic profiling of chronic lymphocytic leukemia identifies subtypes of deletion 13q14. *Cancer Res* 2008; **68**(4)**:** 1012-1021.

22. Negrini M, Cutrona G, Bassi C, Fabris S, Zagatti B, Colombo M*, et al.* microRNAome expression in chronic lymphocytic leukemia: comparison with normal B-cell subsets and correlations with prognostic and clinical parameters. *Clin Cancer Res* 2014; **20**(15)**:** 4141-4153.

23. Calin GA, Cimmino A, Fabbri M, Ferracin M, Wojcik SE, Shimizu M*, et al.* MiR-15a and miR-16-1 cluster functions in human leukemia. *Proc Natl Acad Sci U S A* 2008; **105**(13)**:** 5166-5171.

24. Cimmino A, Calin GA, Fabbri M, Iorio MV, Ferracin M, Shimizu M*, et al.* miR-15 and miR-16 induce apoptosis by targeting BCL2. *Proc Natl Acad Sci U S A* 2005; **102**(39)**:** 13944-13949.

25. Linsley PS, Schelter J, Burchard J, Kibukawa M, Martin MM, Bartz SR*, et al.* Transcripts targeted by the microRNA-16 family cooperatively regulate cell cycle progression. *Mol Cell Biol* 2007; **27**(6)**:** 2240-2252.

26. Allegra D, Bilan V, Garding A, Dohner H, Stilgenbauer S, Kuchenbauer F, *et al.* Defective DROSHA processing contributes to downregulation of MiR-15/-16 in chronic lymphocytic leukemia. *Leukemia* 2014; **28**(1)**:** 98-107.

27. Veronese A, Pepe F, Chiacchia J, Pagotto S, Lanuti P, Veschi S, *et al.* Allele-specific loss and transcription of the miR-15a/16-1 cluster in chronic lymphocytic leukemia. *Leukemia* 2015; **29**(1)**:** 86-95.

28. Mertens D, Wolf S, Tschuch C, Mund C, Kienle D, Ohl S, *et al.* Allelic silencing at the tumor-suppressor locus 13q14.3 suggests an epigenetic tumor-suppressor mechanism. *Proc Natl Acad Sci U S A* 2006; **103**(20)**:** 7741-7746.

29. Raveche ES, Salerno E, Scaglione BJ, Manohar V, Abbasi F, Lin YC, *et al.* Abnormal microRNA-16 locus with synteny to human 13q14 linked to CLL in NZB mice. *Blood* 2007; **109**(12)**:** 5079-5086.

30. Calin GA, Ferracin M, Cimmino A, Di Leva G, Shimizu M, Wojcik SE, *et al.* A MicroRNA signature associated with prognosis and progression in chronic lymphocytic leukemia. *N Engl J Med* 2005; **353**(17)**:** 1793-1801.

31. Underbayev C, Kasar S, Ruezinsky W, Degheidy H, Schneider JS, Marti G, *et al.* Role of mir-15a/16-1 in early B cell development in a mouse model of chronic lymphocytic leukemia. *Oncotarget* 2016.

32. Pekarsky Y, Croce CM. Role of miR-15/16 in CLL. *Cell Death Differ* 2015; **22**(1)**:** 6-11.

33. Morabito F, Cutrona G, Gentile M, Fabris S, Matis S, Vigna E*, et al.* Is ZAP70 still a key prognostic factor in early stage chronic lymphocytic leukaemia? Results of the analysis from a prospective multicentre observational study. *Br J Haematol* 2015; **168**(3)**:** 455-459.

34. Lionetti M, Fabris S, Cutrona G, Agnelli L, Ciardullo C, Matis S*, et al.* High-throughput sequencing for the identification of NOTCH1 mutations in early stage chronic lymphocytic leukaemia: biological and clinical implications. *Br J Haematol* 2014; **165**(5)**:** 629-639.

35. Cutrona G, Colombo M, Matis S, Fabbi M, Spriano M, Callea V*, et al.* Clonal heterogeneity in chronic lymphocytic leukemia cells: superior response to surface IgM cross-linking in CD38, ZAP-70-positive cells. *Haematologica* 2008; **93**(3)**:** 413-422.

36. Durig J, Ebeling P, Grabellus F, Sorg UR, Mollmann M, Schutt P*, et al.* A novel nonobese diabetic/severe combined immunodeficient xenograft model for chronic lymphocytic leukemia reflects important clinical characteristics of the disease. *Cancer Res* 2007; **67**(18)**:** 8653-8661.

37. Bagnara D, Kaufman MS, Calissano C, Marsilio S, Patten PE, Simone R*, et al.* A novel adoptive transfer model of chronic lymphocytic leukemia suggests a key role for T lymphocytes in the disease. *Blood* 2011; **117**(20)**:** 5463-5472.

38. Valdora F, Cutrona G, Matis S, Morabito F, Massucco C, Emionite L*, et al.* A non-invasive approach to monitor chronic lymphocytic leukemia engraftment in a xenograft mouse model using ultra-small superparamagnetic iron oxide-magnetic resonance imaging (USPIO-MRI). *Clin Immunol* 2016.

39. Palamarchuk A, Efanov A, Nazaryan N, Santanam U, Alder H, Rassenti L*, et al.* 13q14 deletions in CLL involve cooperating tumor suppressors. *Blood* 2010; **115**(19)**:** 3916-3922.

40. Kasar S, Salerno E, Yuan Y, Underbayev C, Vollenweider D, Laurindo MF*, et al.* Systemic in vivo lentiviral delivery of miR-15a/16 reduces malignancy in the NZB de novo mouse model of chronic lymphocytic leukemia. *Genes Immun* 2012; **13**(2)**:** 109-119.

41. Fabbri M, Bottoni A, Shimizu M, Spizzo R, Nicoloso MS, Rossi S*, et al.* Association of a microRNA/TP53 feedback circuitry with pathogenesis and outcome of B-cell chronic lymphocytic leukemia. *JAMA* 2011; **305**(1)**:** 59-67.

42. Lin K, Farahani M, Yang Y, Johnson GG, Oates M, Atherton M*, et al.* Loss of MIR15A and MIR16-1 at 13q14 is associated with increased TP53 mRNA, de-repression of BCL2 and adverse outcome in chronic lymphocytic leukaemia. *Br J Haematol* 2014; **167**(3)**:** 346-355.

43. Herling CD, Klaumunzer M, Rocha CK, Altmuller J, Thiele H, Bahlo J*, et al.* Complex karyotypes and KRAS and POT1 mutations impact outcome in CLL after chlorambucil-based chemotherapy or chemoimmunotherapy. *Blood* 2016; **128**(3)**:** 395-404.

44. Rossi D, Rasi S, Spina V, Bruscaggin A, Monti S, Ciardullo C*, et al.* Integrated mutational and cytogenetic analysis identifies new prognostic subgroups in chronic lymphocytic leukemia. *Blood* 2013; **121**(8)**:** 1403-1412.

45. Landau DA, Carter SL, Stojanov P, McKenna A, Stevenson K, Lawrence MS*, et al.* Evolution and impact of subclonal mutations in chronic lymphocytic leukemia. *Cell* 2013; **152**(4)**:** 714-726.

46. Guieze R, Robbe P, Clifford R, de Guibert S, Pereira B, Timbs A*, et al.* Presence of multiple recurrent mutations confers poor trial outcome of relapsed/refractory CLL. *Blood* 2015; **126**(18)**:** 2110-2117.

47. Saleh LM, Wang W, Herman SE, Saba NS, Anastas V, Barber E*, et al.* Ibrutinib downregulates a subset of miRNA leading to upregulation of tumor suppressors and inhibition of cell proliferation in chronic lymphocytic leukemia. *Leukemia* 2016.

48. Calin GA, Liu CG, Sevignani C, Ferracin M, Felli N, Dumitru CD*, et al.* MicroRNA profiling reveals distinct signatures in B cell chronic lymphocytic leukemias. *Proc Natl Acad Sci U S A* 2004; **101**(32)**:** 11755-11760.

49. Visone R, Rassenti LZ, Veronese A, Taccioli C, Costinean S, Aguda BD*, et al.* Karyotype-specific microRNA signature in chronic lymphocytic leukemia. *Blood* 2009; **114**(18)**:** 3872-3879.

50. Pekarsky Y, Santanam U, Cimmino A, Palamarchuk A, Efanov A, Maximov V*, et al.* Tcl1 expression in chronic lymphocytic leukemia is regulated by miR-29 and miR-181. *Cancer Res* 2006; **66**(24)**:** 11590-11593.

51. Bresin A, Callegari E, D'Abundo L, Cattani C, Bassi C, Zagatti B*, et al.* miR-181b as a therapeutic agent for chronic lymphocytic leukemia in the Emicro-TCL1 mouse model. *Oncotarget* 2015; **6**(23)**:** 19807-19818.

52. Visone R, Veronese A, Rassenti LZ, Balatti V, Pearl DK, Acunzo M*, et al.* miR-181b is a biomarker of disease progression in chronic lymphocytic leukemia. *Blood* 2011; **118**(11)**:** 3072-3079.

53. Shah MY, Ferrajoli A, Sood AK, Lopez-Berestein G, Calin GA. microRNA Therapeutics in Cancer - An Emerging Concept. *EBioMedicine* 2016; **12:** 34-42.

Figure legends

Figure 1. Transfection with miRNA mimics and inhibitors and variations in CLL cell viability *in vitro*. (**a**) Expression of miR-15 and miR-16 following transfection with miR-15 (% of positive CLL cells mean±s.e.m.=55.7±5.2) or miR-16 (49.1±7.6) or miR-CTR mimics (10.9±2.2 for miR-15; 10.8±1.9 for miR-16) determined by smartflare technology. Summary of tests on 7 CLL cases with biallelic del(13)(q14) (MG0248, DT0300, MA0088, LD0062, GM0041, RD0296, GD0051).(**b**) Summary of viability determinations obtained on cells from 12 different biallelic del(13)(q14) CLL cases after a 48-h culture following transfection of the indicated miRNA-mimics (data for individual cases are reported in Supplementary Figure S6a). The asterisks indicate data from a CLL case (CG0620) harboring the *TP53* mutation (Supplementary Table S1). (**c**) Expression of miR-15 and miR-16 following transfection with miR-15 (23.17±3) or miR-16 (16.5±2.8) or miR-CTR inhibitors (50.17±6.4 for miR-15; 38.17±4.2 for miR-16). Summary of tests on 6 CLL cases (CP0036, CR0203, PA0145, PM0608, CG0623, MA0342). (**d**) Summary of the viability results obtained on cells from 24 CLL cases transfected with miRNA inhibitors. In (a) and (c) purified CLL cells were transfected with the indicated miRNA mimics or inhibitors and cultured overnight in the presence of miR-15-CY5, miR-16-CY5 or scramble CY5 Smartflare probes. Counter staining with propidium iodide (PI) was employed to evaluate cell viability (see also Supplementary Figure S4). In (b) and (d) viable cells (%) are measured as Annexin-V/PI-double negative cells (Supplementary Figure S5). The *P*-values were obtained by Wilcoxon test in all panels.

Figure 2. CLL cell engraftment in NSG mice following *in vitro* transfection with miRNA mimics or inhibitors. Representative tests on mice engrafted with CLL cells pre-treated *in vitro*

with miRNA mimics (CLL CD0310), miRNA inhibitors (CLL PM0608), or miRNA-CTR. (**a-b**) The figure shows the MRI images 24h after USPIO administration. The position of the spleen is indicated by the dotted red outline. ΔSNR% values also are indicated. The spleens with superior iron uptake and consequent lower ΔSNR% values, appear darker and less nodular. Conversely, spleens with lower iron uptake and higher ΔSNR% values are not so dark and show a nodular structure possibly related to the presence of follicles. Additional explanations are given in text. (**c-d**) α-CD20 Ab staining (red) of paraffin tissue embedded spleen samples following injection of CLL cells pre-treated with the indicated miRNA (**d**). The CD20+ follicle-like structures are highlighted by red squares in (**c**) (magnification 40x). The 400x magnification of a representative follicle for each panel is shown. IHC index is indicated in each panel. (**e-f**) Flow-cytometry analysis of cells from of the same spleens used for the IHC analyses shown in (**c**) and (**d**). CLL cells (CD5+/CD19+) and T cells (CD5+/CD19-) were identified on gated huCD45-positive cells (Supplementary Figure S8). (**e**) Pooled flow-cytometry data obtained from 4 CLL cases with biallelic del(13)(q14) pre-treated with miRNA mimics *in vitro* before injection into mice (n=8 mice for each treatment group). The cells, harvested from mice at the end of tests, were stained and counted. Statistical comparisons were carried out using Wilcoxon-matched pair test. A P-value=0.0078 is indicated by **. (**f**) Pooled flow-cytometry data on cells from 2 CLL cases with normal FISH pre-treated in vitro with miRNA inhibitors prior to injection into mice (n=5 mice for miR-CTR, n=4 for miR-15 and n=5 for miR-16 inhibitors). * and ** indicate P=0.016 and P=0.007 P-values respectively (Mann-Whitney U test). In (**e-f**) values are expressed as mean±s.d. and detailed in Supplementary Table S3.

Figure 3. Effects of *in vivo* treatment with miRNA mimics on CLL cells engrafted in NSG mice. (**a-b**) MRI analysis of the spleen before and after the indicated treatment (representative experiment with cells from MP0456 CLL case). (MRI) images obtained 24 h after Spleens which are characterized by high USPIO uptake appear darker and less granular, a finding which correlates with a low presence of leukemic follicles. See text and legend to Fig. 2 for additional details. (**c**) Summary of MRI results observed on cells from 6 CLL cases biallelic for del(13)(q14) treated with the indicated miRNA mimics. After 2 weeks from CLL cells injection (NSG-CLL, grey dots), mice displayed ΔSNR% values significantly higher compared to those not receiving CLL cells (NSG-CTR, green dots). NSG-CLL mice treated with miR-15 (red dots) or miR-16 (blue dots) mimics had significantly different MRI patterns from the same mice before therapy or after treatment with miR-CTR (black dots). (**d**) Summary of the flow-cytometry analysis of freshly isolated cells from the same spleens analyzed in (c). Percentages of CD19+CD5+ CLLs cells or CD19-CD5+ T cells detected by gating CD45+ cells are expressed as mean±s.d.. (**e**) Summary of the IHC analysis of splenic tissue stained by α-CD20 mAb. In (**c, d, e)** each dot represents an individual mouse. Values also are expressed as mean±s.d.. Statistical comparisons were carried out using Mann-Whitney U test. All data are detailed in Supplementary Table S4.

Figure 4. Effects of treatment with miR-15 or miR-16 mimics on the expansion of CLL clones in NSG mice. (**a-b**) IHC analysis of the spleen of a mouse a representative CLL case (MP0456).The typical CD20+ aggregates (**a**) surrounded by CD3+ T cells (**b**), that are evident in the spleens of the mice treated with miR-CTR, virtually disappear following treatment with miR-15 or miR-16 mimics. 40x magnification view of splenic sagittal sections. The inset indicates the same areas at a higher magnification (400x). (**c**) Numerous cells were stained by α-Cleaved

Caspase 3 mAb in the spleen of mice treated with miR-15. These were virtually absent in mice treated with miR-CTR (magnification 200x and 400x in the inset). (**d**) Summary of flow-cytometry results observed in mice injected with the cells from 6 CLL cases biallelic for del(13)(q14.3). Annexin-V positive cells were determined at the end of the experiment. Each dot represents an individual mouse. Values are expressed as mean±s.d.. Statistical comparisons were carried out using Mann-Whitney U test (****P<0.0001). All data are detailed in Supplementary Table S5.

Figure 5. Effects of treatment with miRNA mimics on the growth of cells from CLL with non-biallelic del(13)(q14. (a) Determination of viable cells (measured as Annexin V/PI-negative cells) in 26 CLL cases at 48-h culture following transfection of the indicated miRNA mimics. CLL cases were grouped according to their karyotype. The asterisks indicate CLL cases carrying TP53 alterations (Supplementary Table S1). (**b**) Summary of the results of the 26 CLLs cases (left panel) and subdivided in cases with monoallelic del(13)(q14) (n=12) (central panel) and with normal FISH (n=9) (right panel). P-values shown were calculated by Wilcoxon test.

793

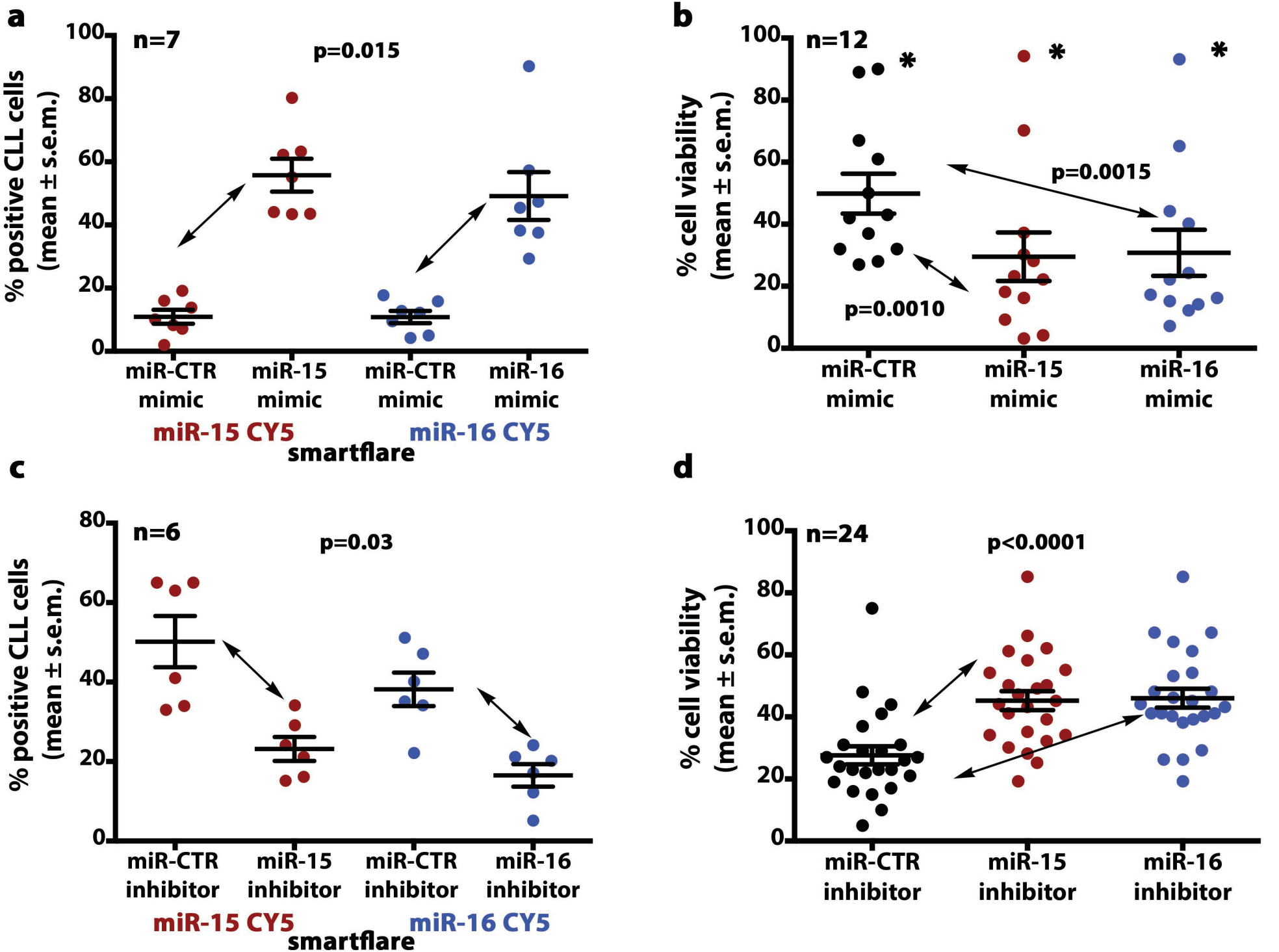
a
n=7
p=0.015
% positive CLL cells
(mean ± s.e.m.)
100
80
60
40
20
0
miR-CTR mimic
miR-15 mimic
miR-CTR mimic
miR-16 mimic
miR-15 CY5
miR-16 CY5
smartflare
b
n=12
% cell viability
(mean ± s.e.m.)
p=0.0015
p=0.0010
miR-CTR mimic
miR-15 mimic
miR-16 mimic
c
n=6
p=0.03
% positive CLL cells
(mean ± s.e.m.)
80
60
40
20
0
miR-CTR inhibitor
miR-15 inhibitor
miR-CTR inhibitor
miR-16 inhibitor
miR-15 CY5
miR-16 CY5
smartflare
d
n=24
p<0.0001
% cell viability
(mean ± s.e.m.)
miR-CTR inhibitor
miR-15 inhibitor
miR-16 inhibitor

Figure 1

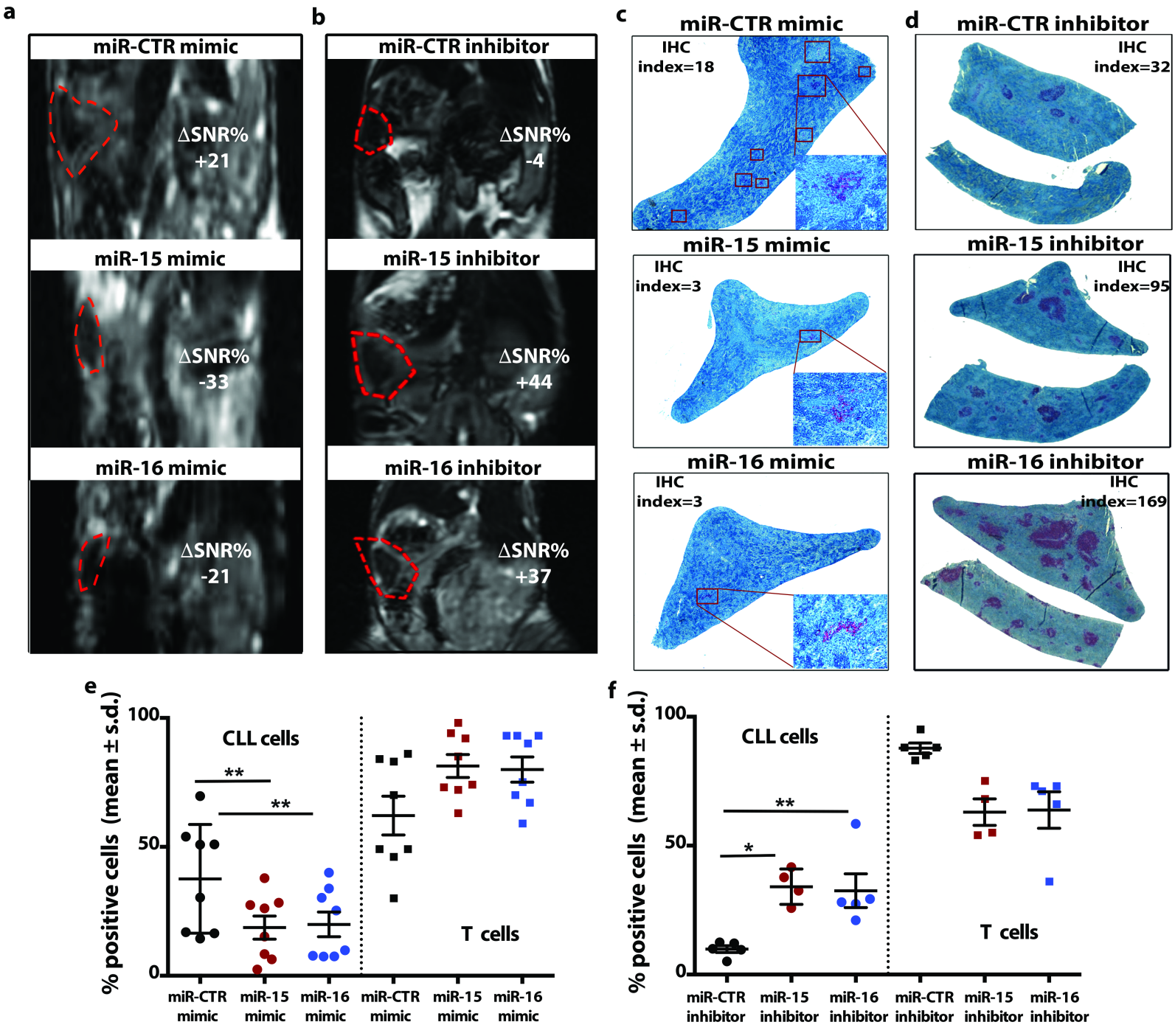
a
b
c
d
miR-CTR mimic
ΔSNR%
+21
miR-15 mimic
ΔSNR%
-33
miR-16 mimic
ΔSNR%
-21
miR-CTR inhibitor
ΔSNR%
-4
miR-15 inhibitor
ΔSNR%
+44
miR-16 inhibitor
ΔSNR%
+37
miR-CTR mimic
IHC
index=18
miR-15 mimic
IHC
index=3
miR-16 mimic
IHC
index=3
miR-CTR inhibitor
IHC
index=32
miR-15 inhibitor
IHC
index=95
miR-16 inhibitor
IHC
index=169
e
% positive cells (mean ± s.d.)
100
50
0
CLL cells
T cells
**
**
miR-CTR mimic
miR-15 mimic
miR-16 mimic
miR-CTR mimic
miR-15 mimic
miR-16 mimic
f
% positive cells (mean ± s.d.)
100
50
0
CLL cells
T cells
**
*
miR-CTR inhibitor
miR-15 inhibitor
miR-16 inhibitor
miR-CTR inhibitor
miR-15 inhibitor
miR-16 inhibitor

Figure 2

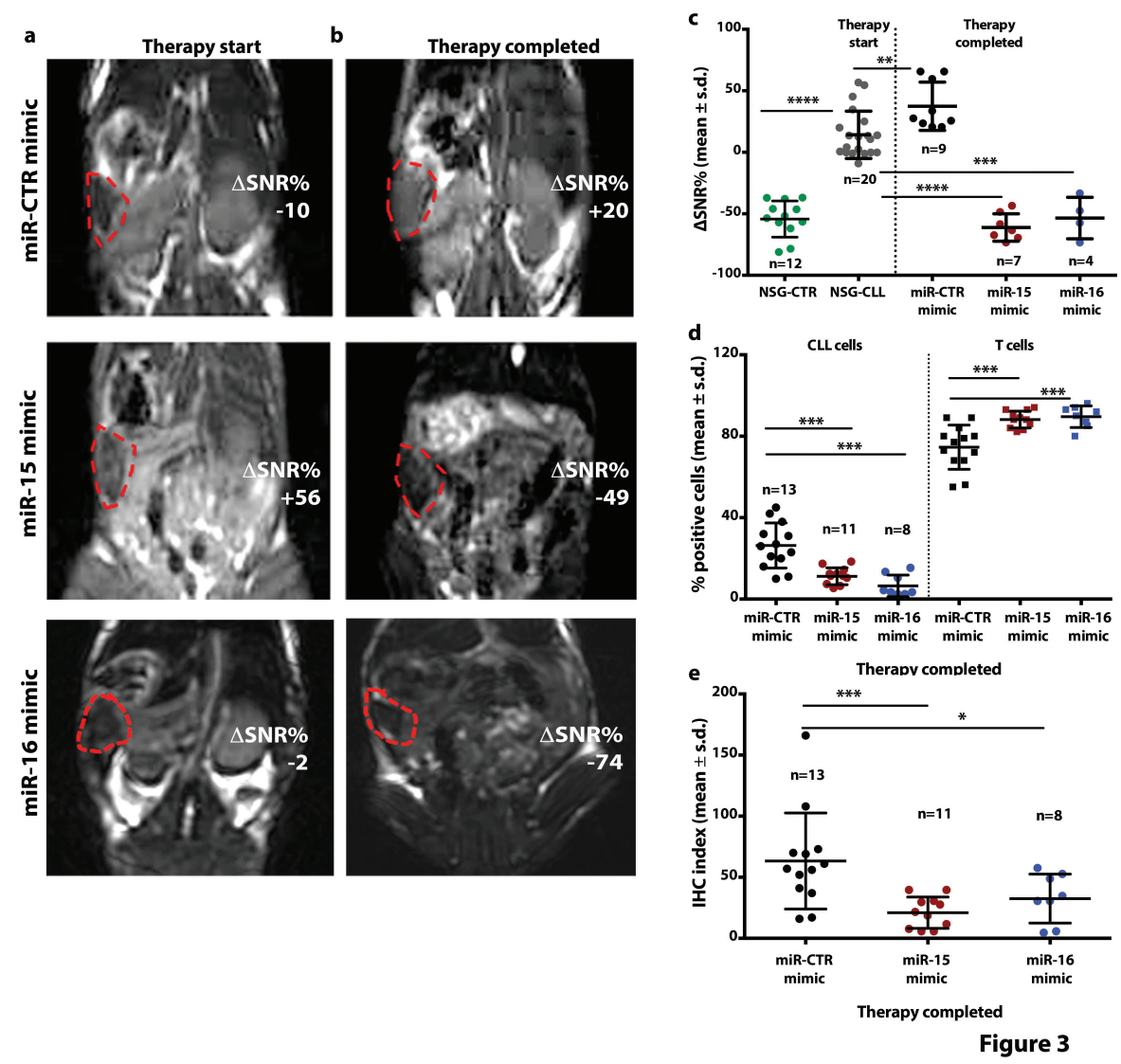
a
Therapy start
b
Therapy completed
miR-CTR mimic
ΔSNR%
-10
ΔSNR%
+20
miR-15 mimic
ΔSNR%
+56
ΔSNR%
-49
miR-16 mimic
ΔSNR%
-2
ΔSNR%
-74
c
Therapy start
Therapy completed
ΔSNR% (mean ± s.d.)
100
50
0
-50
-100
****
**
***
****
n=12
n=20
n=9
n=7
n=4
NSG-CTR
NSG-CLL
miR-CTR mimic
miR-15 mimic
miR-16 mimic
d
CLL cells
T cells
% positive cells (mean ± s.d.)
120
80
40
0
***
***
***
***
n=13
n=11
n=8
miR-CTR mimic
miR-15 mimic
miR-16 mimic
miR-CTR mimic
miR-15 mimic
miR-16 mimic
e
Therapy completed
IHC index (mean ± s.d.)
200
150
100
50
0
***
*
n=13
n=11
n=8
miR-CTR mimic
miR-15 mimic
miR-16 mimic
Therapy completed

Figure 3

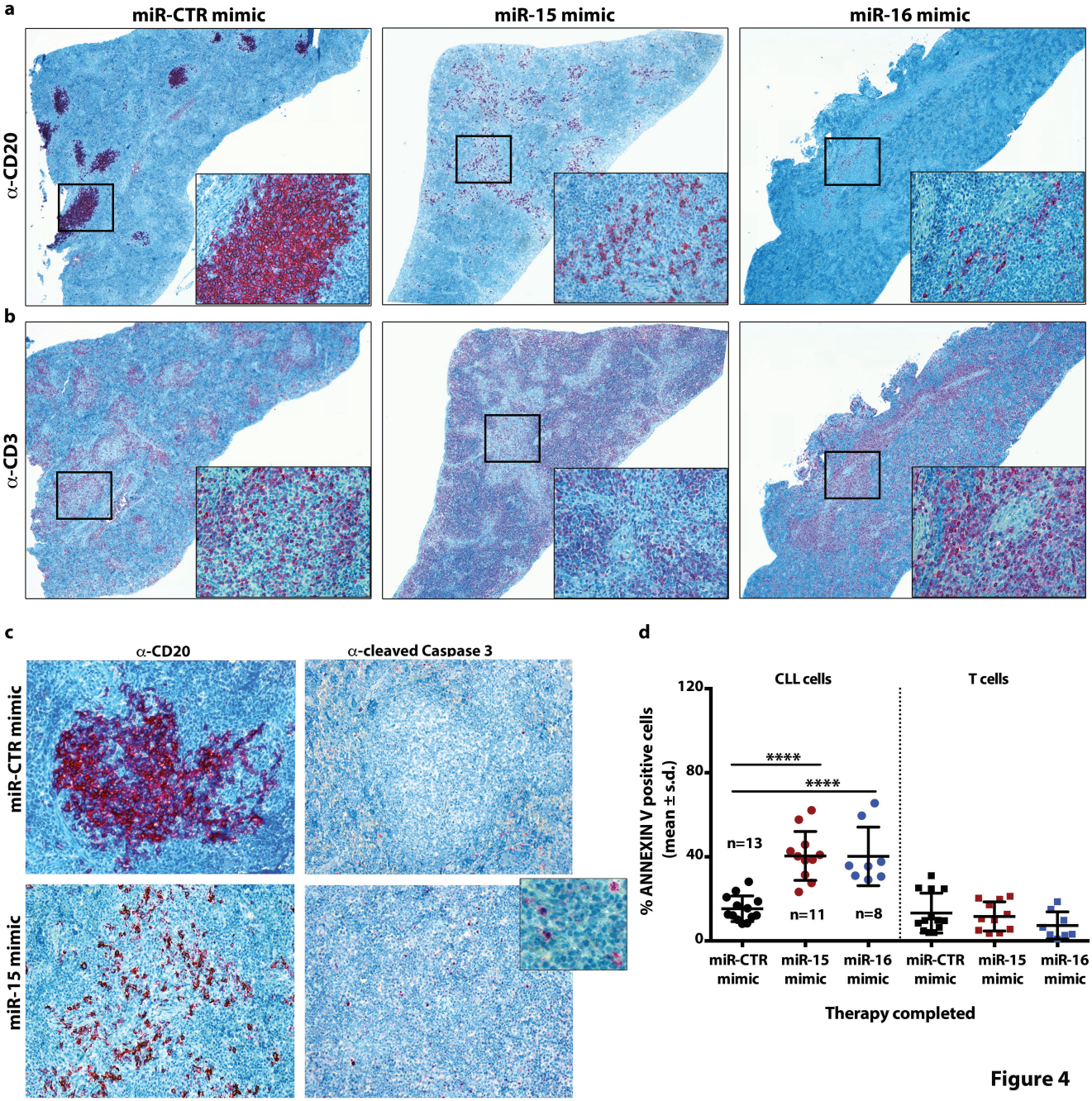
a
miR-CTR mimic
miR-15 mimic
miR-16 mimic
α-CD20
b
α-CD3
c
α-CD20
α-cleaved Caspase 3
miR-CTR mimic
miR-15 mimic
d
CLL cells
T cells
% ANNEXIN V positive cells (mean ± s.d.)
120
80
40
0
****
****
n=13
n=11
n=8
miR-CTR mimic
miR-15 mimic
miR-16 mimic
miR-CTR mimic
miR-15 mimic
miR-16 mimic
Therapy completed

Figure 4

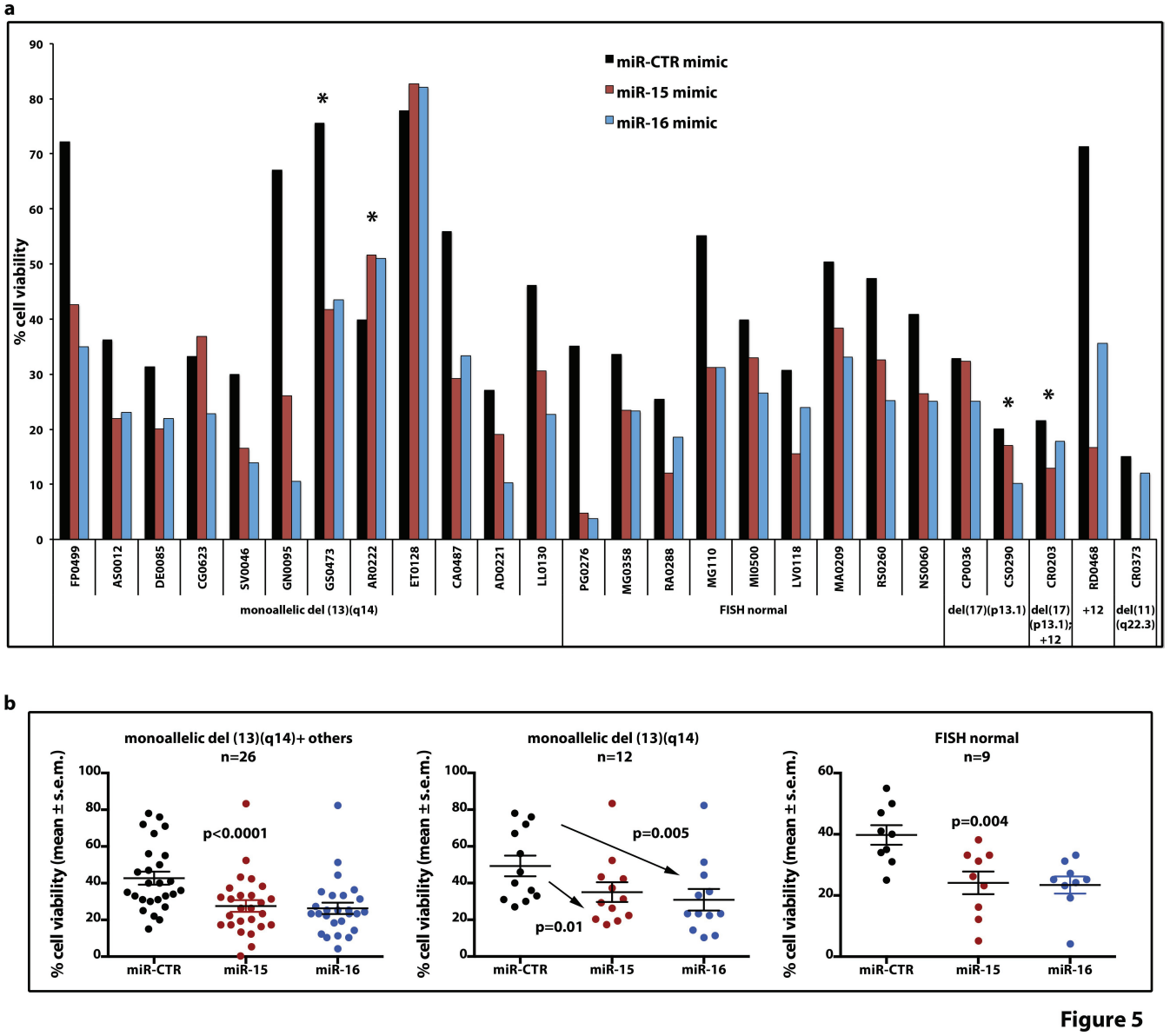
a
% cell viability
miR-CTR mimic
miR-15 mimic
miR-16 mimic
FP0499
AS0012
DE0085
CG0623
SV0046
GN0095
GS0473
AR0222
ET0128
CA0487
AD0221
LL0130
PG0276
MG0358
RA0288
MG110
MI0500
LV0118
MA0209
RS0260
NS0060
CP0036
CS0290
CR0203
RD0468
CR0373
monoallelic del (13)(q14)
FISH normal
del(17)(p13.1)
del(17)(p13.1);+12
+12
del(11)(q22.3)
b
monoallelic del (13)(q14)+ others
n=26
p<0.0001
monoallelic del (13)(q14)
n=12
p=0.005
p=0.01
FISH normal
n=9
p=0.004
% cell viability (mean ± s.e.m.)
miR-CTR
miR-15
miR-16

Figure 5

Table 1. Inhibition of non biallelic del(13q14) CLL cell growth in NSG mice by miR-15 or miR-16 mimic treatment.

ID	miRNAs treatment (n of mice)	CD45+CD19+CD5+ CLL cells (FC) % (mean±s.d.)	CD45+CD19-CD5+ T cells (FC) % (mean±s.d.)	IHC index (mean±s.d.)
FP0499	miR-CTR mimic (3)	9±1.7	90±0.9	137±36.8
	miR-15 mimic (3)	4±0.7	87±2.1	72±10.8
	miR-16 mimic (2)	2±0.3	86±8	26±7.4
GN0095	miR-CTR mimic (2)	13±0.5	82±2.8	107±12.7
	miR-15 mimic (3)	8±1.8	86±2.9	12±10
	miR-16 mimic (3)	7±0.7	82±8.5	23±13.7
RD0468	miR-CTR mimic (4)	13±5.4	51±10.7	56±5.5
	miR-15 mimic (3)	4±1.4	60±2.8	12±5.8
	miR-16 mimic (3)	5±1.5	51±8.4	14±9.8
VS0624	miR-CTR mimic (3)	18±1.9	81±2.7	248±45.1
	miR-15 mimic (3)	8±3.6	87±7.6	68±7.5
	miR-16 mimic (3)	14±1.9	79±6.9	101±35.1
RM0626	miR-CTR mimic (3)	46±12.7	51±15.4	65±12.9
	miR-15 mimic (2)	58±2.5	36±1.4	53±3.5
	miR-16 mimic (2)	63±1.8	28±5.4	53±8.5

FC= flow-cytometry; IHC index= immunohistochemical index.